

Development of shell closures at $N=32,34$. I. β decay of neutron-rich Sc isotopes

S. N. Liddick,^{1,2} P. F. Mantica,^{1,2} R. Broda,³ B. A. Brown,^{1,4} M. P. Carpenter,⁵ A. D. Davies,^{1,4} B. Fornal,³ T. Glasmacher,^{1,4} D. E. Groh,^{1,2} M. Honma,⁶ M. Horoi,⁷ R. V. F. Janssens,⁵ T. Mizusaki,⁸ D. J. Morrissey,^{1,2} A. C. Morton,¹ W. F. Mueller,¹ T. Otsuka,^{9,10} J. Pavan,¹¹ H. Schatz,^{1,4} A. Stolz,¹ S. L. Tabor,¹¹ B. E. Tomlin,^{1,2} and M. Wiedeking¹¹

¹National Superconducting Cyclotron Laboratory, Michigan State University, East Lansing, Michigan 48824, USA

²Department of Chemistry, Michigan State University, East Lansing, Michigan 48824, USA

³Niewodniczanski Institute of Nuclear Physics, PL-31342, Cracow, Poland

⁴Department of Physics and Astronomy, Michigan State University, East Lansing, Michigan 48824, USA

⁵Physics Division, Argonne National Laboratory, Argonne, Illinois 60439, USA

⁶Center for Mathematical Sciences, University of Aizu, Tsuruga, Ikki-machi, Aizu-Wakamatsu, Fukushima 965-8580, Japan

⁷Department of Physics, Central Michigan University, Mount Pleasant, Michigan 48859, USA

⁸Institute of Natural Sciences, Senshu University, Higashimita, Tama, Kawasaki, Kanagawa 214-8580, Japan

⁹Department of Physics, University of Tokyo, Hongo, Tokyo 113-0033, Japan

¹⁰RIKEN, Hirosawa, Wako-shi, Saitama 351-0198, Japan

¹¹Department of Physics, Florida State University, Tallahassee, Florida 32306, USA

(Received 28 July 2004; published 7 December 2004)

Details regarding the β -decay properties of $^{54,55,56}\text{Sc}$ are reported and compared with shell model predictions. The low-energy level structures of even-even $^{54,56}\text{Ti}$ are presented, and the systematic variation of the energy of the first excited 2_1^+ state is discussed in light of proposed shell closures at $N=32,34$ for the neutron-rich Ti isotopes.

DOI: 10.1103/PhysRevC.70.064303

PACS number(s): 23.40.-s, 23.20.Lv, 27.40.+z, 21.60.Cs

I. INTRODUCTION

The low-energy structure of neutron-rich nuclei with nucleons occupying the $\pi f_{7/2}-\nu pf$ shell model orbitals is affected dramatically by the strong and attractive proton-neutron monopole interaction between the spin-orbit partner orbitals $\pi f_{7/2}$ and $\nu f_{5/2}$. As protons are added to the $\pi f_{7/2}$ orbital, the effective single-particle energy of the $\nu f_{5/2}$ orbital decreases significantly relative to other members of the νpf shell. The monopole migration of the $\nu f_{5/2}$ orbital, in combination with the large spin-orbit splitting between $\nu p_{3/2}$ and $\nu p_{1/2}$, leads to the development of an $N=32$ subshell gap for nuclides in which the $\pi f_{7/2}$ orbital is occupied by four or fewer protons.

Early evidence for a subshell closure at $N=32$ was seen in the Ca isotopes, where both the mass [1] and relatively high value of the excitation energy of the first excited 2^+ [$E(2_1^+)$] in ^{52}Ca [2] suggested added stability. However, systematic data for isotopes beyond ^{52}Ca were unavailable, and it was believed that the appearance of a subshell gap at $N=32$ was reinforced by the proton shell closure at $Z=20$ [3]. Experimental evidence for a potential subshell closure at $N=32$ for the ^{24}Cr isotopes was reported in Ref. [4], based on the systematic variation of $E(2_1^+)$ in the even-even Cr isotopes. The value $E(2_1^+)=1007$ keV of $^{56}\text{Cr}_{32}$ is more than 100 keV above that observed in neighbors $^{54,58}\text{Cr}$. The systematic behavior of $E(4_1^+)/E(2_1^+)$ in the Cr isotopes is also suggestive of a subshell closure at $N=32$ [5].

The systematic variation of $E(2_1^+)$ along the $N=32$ isotonic chain was completed for the $\pi f_{7/2}$ nuclides with the determination of $E(2_1^+)=1495$ keV for ^{54}Ti [6]. The increase in $E(2_1^+)$ from ^{24}Cr to ^{20}Ca with the removal of protons from the $f_{7/2}$ orbital, as shown in Fig. 1, parallels the expected

growth of the single-particle energy gap at $N=32$ due to the monopole migration of the $\nu f_{5/2}$ orbital. The high-spin data available for the even-even $^{50,52,54}\text{Ti}$ isotopes provide additional evidence for the $N=32$ gap [6]. In ^{54}Ti , the significant spacing between the 6_1^+ state at 2936 keV and the cluster of levels 8_1^+ , 9_1^+ , and 10_1^+ at ~ 5800 keV suggests that a substantial energy gap must be overcome when promoting one of the coupled $\nu p_{3/2}$ neutrons to either the $\nu p_{1/2}$ or the $\nu f_{5/2}$.

It was predicted [7] that the continued monopole shift of the $\nu f_{5/2}$ orbital may also lead to the development of a shell closure at $N=34$ and that the low-energy structure of ^{54}Ca may show similarities to that of ^{48}Ca , which is doubly magic. The shell model calculations by Honma *et al.* employed a new effective shell model interaction, designated GXPF1, which is based on effective two-body matrix elements with some replacement by the G matrix [7,8]. The onset of an $N=34$ shell closure was first expected to be evident in the Ti isotopes, where $E(2_1^+)$ for $^{56}\text{Ti}_{34}$ was predicted to lie at approximately 1500 keV, similar in energy to its neighbor $^{54}\text{Ti}_{32}$. We have recently reported the energy of the 2_1^+ state in

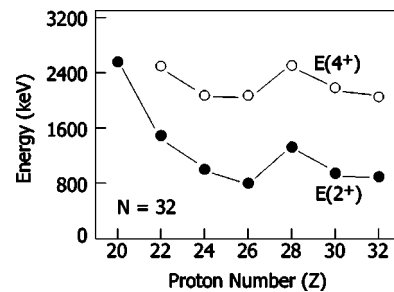


FIG. 1. Systematic variation of $E(2_1^+)$ and $E(4_1^+)$ for the $N=32$ isotones.

^{56}Ti at 1127 keV [9], which is nearly 400 keV below that derived from shell model calculations using the GXPF1 interaction and midway between the shell model predictions using GXPF1 and KB3G [10]. The relatively low value of $E(2_1^+)$ for ^{56}Ti suggests that a significant $\nu p_{1/2}-\nu f_{5/2}$ gap has not yet developed at $Z=22$.

The low-energy structures of $^{54,56}\text{Ti}$ populated in β decay were first reported in Refs. [6,9]. In this paper, we present details of the β -decay properties of the neutron-rich $^{54,55,56}\text{Sc}$ isotopes, which populate low-energy states in $^{54,55,56}\text{Ti}$, respectively. The deduced absolute β -decay branching ratios to the even-even daughter states for the decay of the odd-odd $^{54,56}\text{Sc}$ are used to assign spins and parities to the ground states of the decay parents. The general trend in the monopole shift of the $\nu f_{5/2}$ orbital is tracked by examining the ground-state spin and parity assignments for the odd-odd V and Sc nuclides, employing the extreme single-particle model with the assumption that $N=32$ is a good subshell closure. The absence of a shell closure at $N=34$ for the Ti isotopes as predicted by Ref. [7] is discussed, along with the implication these new results have on the low-energy structure of the neighboring Ca isotopes and other neutron-rich nuclides in the $\pi f_{7/2}-\nu pf$ shell region.

II. EXPERIMENTAL TECHNIQUE

The β -decay properties of the neutron-rich $^{54,55,56}\text{Sc}$ parent nuclides were deduced in two separate experiments carried out using the experimental facilities at the National Superconducting Cyclotron Laboratory (NSCL) at Michigan State University. Results from the first of these two experiments have been published previously [6,11,12], and details regarding the experimental methods are given in Ref. [11]. Data were collected for the decays of $^{54,55}\text{Sc}$ during the first measurement. The decay of ^{56}Sc was studied in a second experiment, where many of the methods employed in the first experiment were also utilized. The discussion below provides an overview regarding the experimental techniques applied to both measurements, highlighting specific differences between the two, which aimed mostly at enhancing the detection efficiencies for both β and γ rays to counteract the decreasing production cross section for the more neutron-rich ^{56}Sc .

A 140-MeV/nucleon $^{86}\text{Kr}^{34+}$ beam was produced using the coupled cyclotrons at the NSCL. The average beam current on target was 3 pA in the first experiment, and 15 pA during the second. The ^{86}Kr beam was fragmented in a 376-mg/cm²-thick Be target located at the object position of the A1900 fragment separator [13]. The secondary fragments of interest were selected in the A1900 using a 330-mg/cm² Al degrader and 1% momentum slits; both were located at the intermediate image of the device.

The fully stripped fragments were implanted in a double-sided Si microstrip detector (DSSD) that is part of the NSCL β counting system [14]. The DSSD thickness was 985 μm in the first experiment and 1470 μm in the second. Fragments were unambiguously identified by a combination of multiple energy loss signals and time of flight. The desired Sc fragments were selected using three different A1900 magnetic

rigidity settings: 1.3×10^4 ^{54}Sc implants were collected with the A1900 set to $B\rho_1=4.042$ Tm and $B\rho_2=3.755$ Tm, 2.4×10^3 ^{55}Sc implants with $B\rho_1=4.126$ Tm and $B\rho_2=3.842$ Tm, and 1.3×10^4 ^{56}Sc implants with $B\rho_1=4.239$ Tm and $B\rho_2=3.944$ Tm. At each A1900 rigidity settings, the desired Sc fragments were less than 1% of the total composition of the secondary beam. Representative particle identification spectra for the $^{54,55}\text{Sc}$ rigidity settings are available in Ref. [11].

Fragment- β correlations were established in software by requiring a high-energy implant event in a single pixel of the DSSD followed by a low-energy β event in the same pixel. For the ^{56}Sc data analysis, due to the overall low implantation rate (<15 s⁻¹) into the DSSD, the correlation was expanded to also include implant events that occurred in the nearest eight neighbors of the pixel recording a β -decay event. The differences between the absolute time stamps of correlated β and implant events were histogrammed to generate a decay curve. To suppress background, implants were rejected if they were not followed by a β event within a specified time period in the same pixel or if they were followed by a second implantation within the same specified time period, also within the same pixel. The time periods were selected based on the decay half-life of the fragment of interest. For the decays of $^{54,55}\text{Sc}$, the specified time period was 10 s, while for the ^{56}Sc decay this time was reduced to 1 s. β -detection efficiencies were 30%, 40%, and 30% for $^{54,55,56}\text{Sc}$, respectively. The efficiencies reflect in part an improved correlation efficiency with the decrease in overall particle implant rate into the DSSD.

Delayed γ rays were measured using Ge detectors from the MSU Segmented Germanium Array (SeGA) [15] arranged around the β counting system. During the first experiment, six Ge detectors were deployed, providing a peak efficiency for γ -ray detection of 3.3% at 1 MeV. Six additional detectors were placed around the β counting system for the ^{56}Sc measurement, giving a total peak detection efficiency of 5.3% at 1 MeV. The energy resolution for each of the Ge detectors was measured to be ~ 3.5 keV for the 1.3 MeV γ -ray transition in ^{60}Co .

III. RESULTS

A. ^{54}Sc

The β -delayed γ -ray spectra for ^{54}Sc in the range 0 to 2 MeV, shown in Fig. 2, contain $\beta\gamma$ events that occurred (a) within the first 10 s and (b) within the first 1 s after a ^{54}Sc implant. Three transitions at 1001, 1021, and 1495 keV persist in both spectra and have been assigned to the β decay of ^{54}Sc . Sorlin *et al.* [16] had previously assigned transitions at 500 ± 50 , 1000 ± 50 , and 1700 ± 50 keV with absolute intensities of 40 ± 20 , 50 ± 20 , and 40 ± 20 , respectively, to the decay of ^{54}Sc .

The decay curve derived from ^{54}Sc -correlated β decays is shown in Fig. 3. The curve was fitted considering a single-exponential decay of the parent ^{54}Sc , exponential growth and decay of the daughter ^{54}Ti , and an exponential background component. The decay constant for the exponential back-

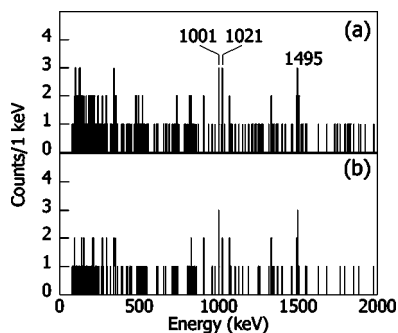


FIG. 2. β -delayed γ -ray spectra for ^{54}Sc in the range 0–2 MeV. The spectra include events within the first (a) 10 s and (b) 1 s after a ^{54}Sc implant. The peaks labeled by energy have been identified as transitions in ^{54}Ti following the decay of ^{54}Sc .

ground of 0.144 s^{-1} was deduced by fitting the decay curves for all nuclides implanted along with ^{54}Sc as described in Ref. [11]. The deduced half-life for the decay of ^{54}Sc is $360\pm 60\text{ ms}$, which is in disagreement with a previous measurement of $225\pm 40\text{ ms}$ by Sorlin *et al.* [16]. The uncertainty of the known half-life of the daughter ^{54}Ti [17], $1.5\pm 0.4\text{ s}$, contributed significantly to the uncertainty of the half-life of ^{54}Sc reported here. The presence of a β -decaying isomer in ^{54}Sc cannot be ruled out experimentally. The limited statistics of the experiment did not permit gating of the decay curve on individual γ -ray transitions assigned to ^{54}Sc decay. However, the existence of a μs isomeric transition in ^{54}Sc [18] and the expected ordering of the low-energy states as predicted by the shell model (see Discussion section) are not supportive of a β -decaying isomer in ^{54}Sc .

The proposed decay scheme for levels in ^{54}Ti populated following the β decay of ^{54}Sc is shown in Fig. 4. The β -decay Q value was derived from the measured mass excess of both parent and daughter as compiled in Ref. [19]. Absolute γ -ray intensities were deduced from the number of observed ^{54}Sc β -delayed γ rays, the simulated γ -ray efficiency curve [11], and the number of ^{54}Sc implants correlated with β decays. The last term was derived from the fit of

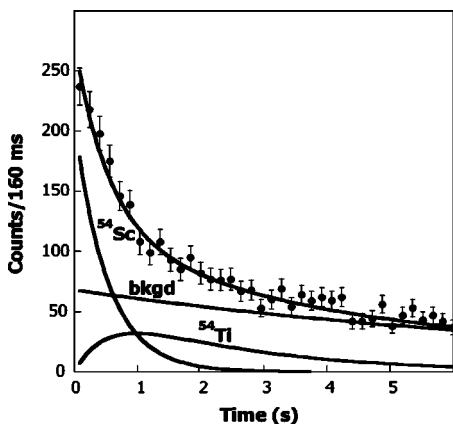


FIG. 3. Decay curve for ^{54}Sc . Data were fitted with a single-exponential decay and the exponential growth and decay of the short-lived daughter ^{54}Ti . An exponential background is also considered in the fit. See text for details.

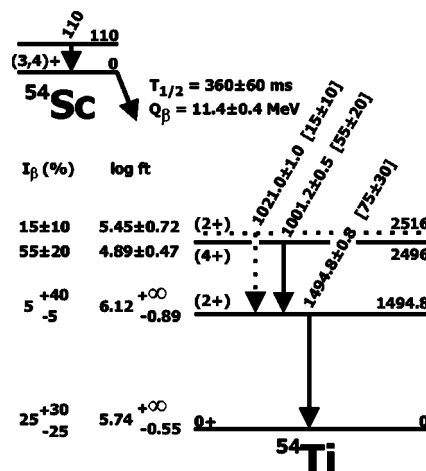


FIG. 4. Proposed level scheme for ^{54}Ti populated following the β decay of ^{54}Sc . The number in brackets following the γ -ray-decay energy is the absolute γ -ray intensity in percent. The Q_β value was deduced from data in Ref. [19].

the decay curve in Fig. 3. The 1495-keV transition has the largest absolute intensity and was tentatively identified as the $2_1^+ \rightarrow 0_1^+$ transition in ^{54}Ti [6]. It was not possible to derive information regarding $\gamma\gamma$ coincidences due to the marginal statistics observed in the γ -ray spectrum for ^{54}Sc . However, based on the derived absolute intensities, the 1001- and 1021-keV γ -ray transitions were placed so as to feed the proposed 2_1^+ state at 1495 keV.

Assignment of the 1495-keV γ ray to a transition in ^{54}Ti permitted a detailed evaluation of $\gamma\gamma\gamma$ matrices derived from prompt γ rays observed following the deep-inelastic collisions of ^{48}Ca projectiles with a ^{208}Pb target [6]. As a result, yrast transitions up to $J^\pi=10^+$ have been identified in ^{54}Ti . The 1495- and 1001-keV γ rays were confirmed as the $2_1^+ \rightarrow 0_1^+$ and $4_1^+ \rightarrow 2_1^+$ transitions, respectively. The 1021-keV transition was not observed in the prompt γ -ray spectrum recorded following the deep-inelastic reaction. Therefore, we assume that the 1021-keV transition is not part of the yrast cascade and have tentatively assigned $J^\pi=2^+$ to the 2516-keV level in ^{54}Ti .

Apparent β feedings and $\log ft$ values to levels in ^{54}Ti are reported in Fig. 4 and were deduced from the absolute γ -ray intensities. Direct β feeding to the 4^+ level would limit the spin and parity of the ground state of ^{54}Sc to $J^\pi=3^+, 4^+$, or 5^+ . The apparent β feeding to the ^{54}Ti ground state includes zero within experimental errors, supporting $J \geq 2$ for the ground state of ^{54}Sc . Absence of the known $6_1^+ \rightarrow 4_1^+$ transition at 439 keV [6] in the β -delayed γ -ray spectrum reduces the range of possible J^π values to 3^+ or 4^+ for the ground state of ^{54}Sc .

The β counting system, as deployed, could also be used to identify microsecond isomers in the nuclides which composed the secondary beam. γ rays occurring within a 20- μs window after a fragment implant into the DSSD were recorded in the data stream. The isomeric γ -ray spectrum in coincidence with ^{54}Sc implants is shown in Fig. 5. Assignment of a 110-keV isomeric transition to ^{54}Sc was first proposed by Grzywacz *et al.* [18]. The 110-keV transition was

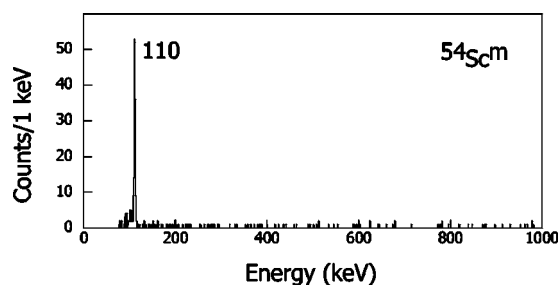


FIG. 5. γ -ray spectrum collected within a 20- μ s time window after a ^{54}Sc implant. The 110-keV isomeric transition was previously reported in Ref. [18].

assigned $E2$ multipolarity, based on Weisskopf estimates that considered the deduced lifetime and transition energy. Grzywacz *et al.* tentatively assigned $J^\pi=5^+$ to the isomeric state in ^{54}Sc ; however, based on the transition multipolarity and the possible J^π assignments for the ^{54}Sc ground state, the J assignment for the isomer could be as low as $J=1$ or as high as $J=6$.

B. ^{55}Sc

The decay curve derived from ^{55}Sc -correlated β decays is shown in Fig. 6(a). The curve was fitted considering a single-exponential decay for the parent ^{55}Sc , exponential growth and decay of the daughter ^{55}Ti with half-life 1.3 ± 0.1 s [12], and an exponential background component. The decay constant for the exponential background of 0.0815 s $^{-1}$ was deduced by fitting the decay curves for all nuclides implanted along with ^{55}Sc , again as described in Ref. [11]. The deduced half-life for the decay of ^{55}Sc was 115 ± 15 ms, which compares well with the value of 120 ± 40 ms reported by Sorlin *et al.* [16].

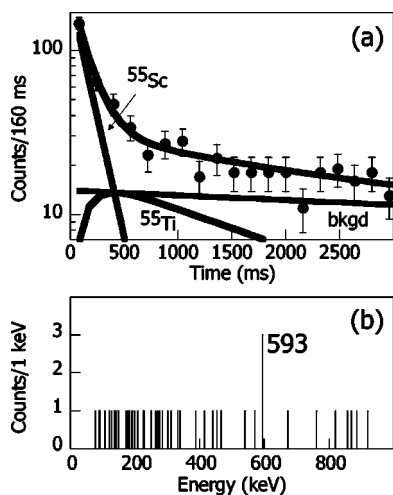


FIG. 6. (a) Decay curve for ^{55}Sc . Data were fitted with a single-exponential decay and the exponential growth and decay of the short-lived daughter ^{55}Ti . An exponential background is also considered in the fit. (b) β -delayed γ -ray spectrum for ^{55}Sc in the range 0–1.0 MeV. A gate was placed on the decay curve to include only events within the first second of a ^{55}Sc implant.

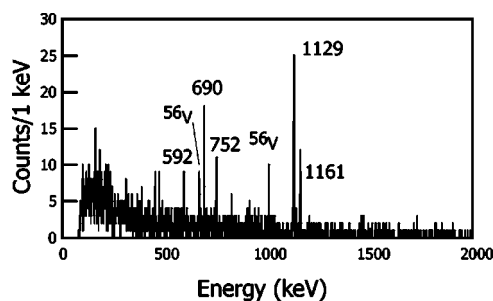


FIG. 7. β -delayed γ -ray spectrum for ^{56}Sc in the range 0–2 MeV. This spectrum includes events within the first second after a ^{56}Sc implant.

A single transition at 593 ± 1 keV was observed in the β -delayed γ -ray spectrum for ^{55}Sc shown in Fig. 6(b). The absolute intensity of this single transition, assigned to the decay of ^{55}Sc , was deduced to be $(40 \pm 20)\%$.

C. ^{56}Sc

The β -delayed γ -ray spectrum for ^{56}Sc in the range of 0 to 2 MeV, shown in Fig. 7, contains $\beta\gamma$ events that occurred within the first second after a ^{56}Sc implant. A total of seven transitions have been identified in this spectrum. The analysis differs from that in Ref. [9] in two ways. First, as a result of the small mismatch between the energy of the ^{56}V daughter reported in Ref. [9] and that in Ref. [11], the Ge energy calibration was improved. Second, in the work reported here, multiple β particles, due to daughter decays along the isobaric chain, were correlated with a single implant if they occurred within the 1-s fragment- β correlation time. These two changes to the data analysis routine resulted in both a better match with previously reported energies and an increase in the observed daughter and granddaughter activities compared to the results reported in Ref. [9]. This is evident from the increased peak areas for the γ rays assigned to the granddaughter ^{56}V at 668.2 ± 0.6 and 1006.4 ± 0.4 keV in Fig. 7. As the decay of ^{56}Ti has no known γ -ray transitions [12], the five remaining transitions have been assigned to the β decay of ^{56}Sc and are listed in Table I. The transitions located at 690.2 ± 0.4 , 1128.2 ± 0.4 , and 1160.0 ± 0.5 keV compare favorably with the energies of 690.0 ± 0.5 , 1128.8 ± 0.5 , and 1161.0 ± 0.5 keV found in deep-inelastic work reported in the accompanying paper [20]. The weighted averages of the β -decay and in-beam results, 690.1 ± 0.4 , 1128.5 ± 0.4 , and 1160.5 ± 0.5 keV, have been adopted as the energies for these three γ -ray transitions in ^{56}Ti . The most intense transition in the $\beta\gamma$ spectrum is located at 1129 keV and has been tentatively identified as the $2_1^+ \rightarrow 0_1^+$ transition [9]. The γ -ray transition with energy 592.3 ± 0.5 falls within the error of the single γ -ray transition observed in ^{55}Ti and could be due to a β -delayed neutron branch from ^{56}Sc to levels in ^{55}Ti . Such a branch is feasible considering that the 13.7 ± 0.8 MeV Q value for the ^{56}Sc β decay is considerably larger than the 5.3 ± 0.3 MeV neutron separation energy in ^{56}Ti .

The decay curve derived from ^{56}Sc -correlated β decays is given in Fig. 8(a). The decay curves obtained by requiring an additional coincidence with the 1129-, 690-, or

TABLE I. γ -ray transitions in ^{56}Ti identified following the β decay of ^{56}Sc . The adopted energies are a weighted average of results from β -decay and in-beam experiments [20]. See text for details.

$E_{\gamma}, \beta\text{-decay(keV)}$	E_{γ} adopted(keV)	$I_{\gamma}^{\text{abs}}(\%)$	Initial state (keV)	Final state (keV)
592.3 ± 0.5	592.3 ± 0.5	7 ± 2		
690.2 ± 0.4	690.1 ± 0.4	19 ± 4	2980	2290
751.5 ± 0.5	751.5 ± 0.5	9 ± 3		
1128.2 ± 0.4	1128.5 ± 0.4	48 ± 11	1129	0
1160.0 ± 0.5	1160.5 ± 0.5	21 ± 5	2290	1129

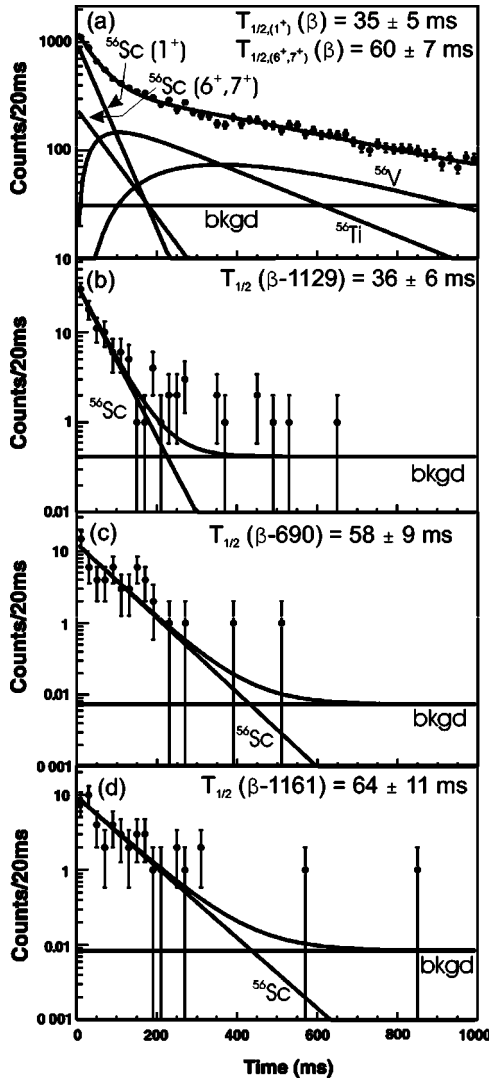


FIG. 8. Decay curves for ^{56}Sc , showing (a) fragment- β correlations only, where the data were fitted with an exponential decay from the ^{56}Sc ground state and isomeric state, with weights of 83% and 20%, respectively, and ^{56}Ti and ^{56}V growth and decay with a linear background; (b) fragment- β correlations with an additional requirement of a 1129-keV γ ray in coincidence; (c) fragment- β correlations with an additional requirement of a 690-keV coincident γ ray; and (d) fragment- β correlations with an additional requirement of the presence of a 1161-keV γ ray. The curves shown in (b), (c), and (d) were fitted with a single exponential and constant background.

1161-keV β -delayed γ rays are given in Figs. 8(b)–8(d). The half-life deduced from the 1129-keV γ -gated decay curve is statistically different from those deduced from the 690- and 1161-keV γ -gated decay curves, suggesting that two β -decaying states were populated in the production of ^{56}Sc . A weighted average of the half-lives extracted from the 690- and 1161-keV γ -gated decay curves results in a value of 60 ± 7 ms, which is adopted for the higher-spin β -decaying state in the ^{56}Sc parent. Since the 1129-keV γ ray has been tentatively assigned to the $2_1^+ \rightarrow 0_1^+$ transition, it appears that the lower-spin ^{56}Sc state has a shorter half-life and that the 1129-keV γ -gated decay curve is then a mixture reflecting both the low- and high-spin state half-lives. The percentages of β decays due to the low- and high-spin states are $(83 \pm 11)\%$ and $(20 \pm 4)\%$, respectively, based on absolute γ -ray intensities and the deduced β feeding to the ^{56}Ti ground state.

The ^{56}Sc -correlated β decay curve, Fig. 8(a), was first fitted using a single-exponential decay component for ^{56}Sc with daughter and granddaughter generations. The resulting half-life is consistent with the previous determination [9]. However, evidence for two β -decaying states in ^{56}Sc resulted in a reexamination of the overall fragment- β decay curve. Since the half-life of the high-spin β -decaying state was extracted from the decay curves gated on the 690- and 1161-keV γ -ray transitions, the value for the low-spin half-life can be deduced from the total β decay half-life curve. The decay curve in Fig. 8(a) was fitted to a function that considered the high-spin state half-life, along with the percentage of β decays attributed to the high- and low-spin states, the exponential growth and decay of the daughter and granddaughter isotopes, ^{56}Ti [12] and ^{56}V [11], and a linear background component. In this way, a half-life of 35 ± 5 ms was deduced for the lower-spin state in ^{56}Sc . The isotopes $^{58,59}\text{V}$, ^{57}Ti , and ^{60}Cr , which have previously measured half-lives, were implanted along with ^{56}Sc . The decay curves for these four isotopes were also fitted and used to verify the linear background.

The isomeric γ -ray spectrum collected within a 20- μs time window following a ^{56}Sc implant is shown in Fig. 9. Three transitions were observed at 140 ± 2 , 188 ± 2 , and 587 ± 2 keV with absolute γ -ray intensities of $(1.4 \pm 0.1)\%$, $(1.8 \pm 0.3)\%$, and $(2.2 \pm 0.6)\%$, respectively. It is possible that the 587-keV line observed in Fig. 9 is doublet. Unfortunately, the errors in the absolute intensities and the lack of coincidence data do not permit the placement of any of the three isomeric transitions in the low-energy structure of ^{56}Sc at the present time.

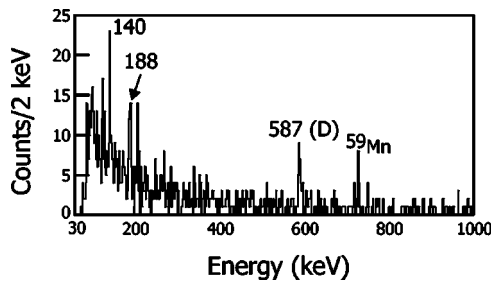


FIG. 9. γ -ray spectrum collected within a 20- μ s time window following a ^{56}Sc implant. The 587-keV transition is a possible doublet.

The proposed decay scheme for levels in ^{56}Ti populated following the β decay of ^{56}Sc is shown in Fig. 10. Details of the γ -ray placements and spin and parity assignments were aided by a complementary experiment carried out at the ATLAS accelerator at Argonne National Laboratory with the Gammasphere multidetector array to study the yrast structure of neutron-rich Ti isotopes as described in detail in the accompanying paper [20]. Note that the placement of the 690-keV γ -ray feeding the 1129-keV state in ^{56}Sc was also confirmed by fragment- $\beta\gamma\gamma$ coincidences (see Fig. 11). The

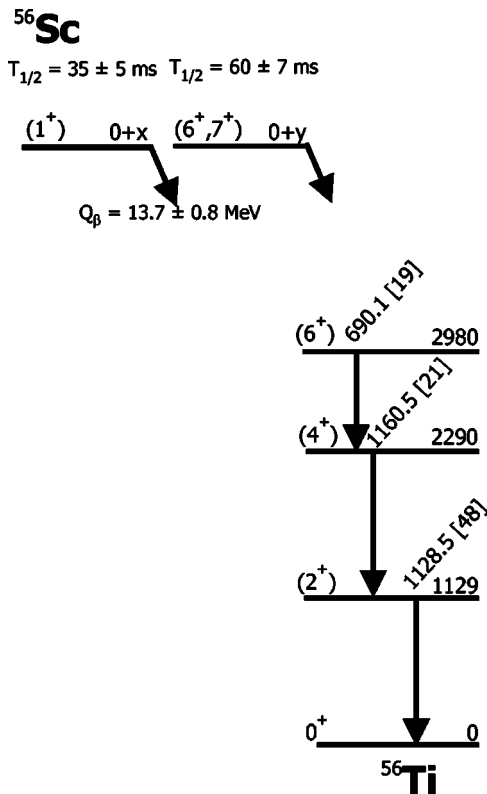


FIG. 10. Proposed level scheme for ^{56}Ti populated following the β decay of ^{56}Sc . The decay energies are the adopted values taken from a weighted average of the β -decay and in-beam experiments discussed in the text. The number in brackets following the γ -ray-decay energy is the absolute γ -ray intensity in percent. The Q_β value was deduced from data in Ref. [19]. A possible β -delayed neutron branch precludes the determination of β -branching ratios to ^{56}Ti excited states.

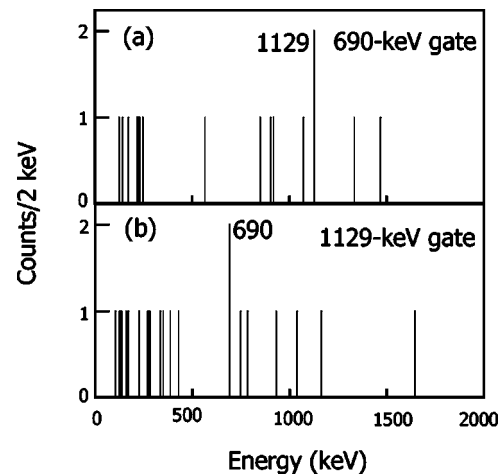


FIG. 11. γ rays in coincidence with the (a) 690-keV and (b) 1129-keV γ -ray transitions following ^{56}Sc β decay.

β -decay Q value was derived from the mass excess of both parent and daughter as compiled in Ref. [19]. Absolute γ -ray intensities were deduced from the number of observed ^{56}Ti γ rays, the simulated γ -ray efficiency curve, and the number of ^{56}Sc implants correlated with β decays. The last term was derived from a fit of the decay curve in Fig. 8(a).

Apparent β -decay branching ratios are not presented in Fig. 10 due to the possible presence of a β -delayed neutron branch following the decay of ^{56}Sc . An apparent ground-state β -decay branch was deduced from the difference between the total number of β decays and the observed γ -ray intensity depopulating the 2_1^+ state. β -decay branching to the ^{56}Ti ground and first excited 2^+ state of ^{56}Ti led to the tentative assignment of 1^+ to the spin and parity of the parent ^{56}Sc low-spin isomer. Apparent direct feeding to the 6^+ , 2980-keV level in ^{56}Ti from the high-spin ^{56}Sc isomer limits the spin of the high-spin isomeric state to values of 5, 6, or 7. The absence of direct β feeding to the 4_1^+ state (the absolute intensities of the 690- and 1161-keV transitions are equivalent within experimental errors) further restricts the spin of the ^{56}Sc high-spin β -decaying isomer to $J=(6, 7)$.

IV. DISCUSSION

A. Comparison with shell model results

The low-energy structures of the even-even $_{24}\text{Cr}$, $_{22}\text{Ti}$ and $_{20}\text{Ca}$ isotopes beyond the $N=28$ shell closure have previously been compared [9] to the results of shell model calculations employing the GXPF1 [7,8] and KB3G [10] interactions. Both calculations were shown to reproduce the observed increase in the $E(2_1^+)$ values at $N=32$ for the Cr, Ti, and Ca isotopes. The presence of a subshell closure at $N=32$ can be attributed to a gap in the effective single-particle energies between $\nu p_{3/2}$ and $\nu f_{5/2}$ states created by the monopole migration of the $\nu f_{5/2}$ as protons are removed from the $f_{7/2}$ orbital. Such dramatic changes in effective single-particle energies due to strongly attractive interactions between spin-orbit coupling partners have been discussed by Otsuka *et al.* [21] in the context of the disappearing $N=8, 20$ magic num-

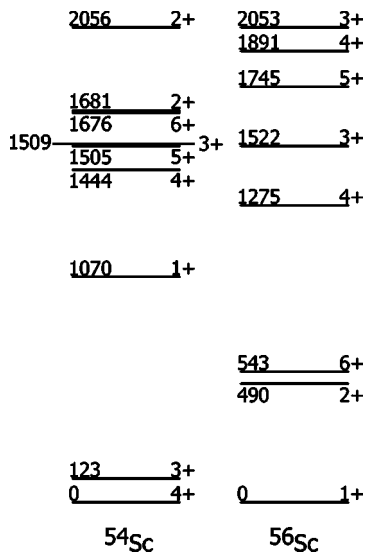


FIG. 12. Low-energy levels of $^{54,56}\text{Sc}$ calculated in the full pf -shell model space using the GXPF1 interaction.

bers for neutron-rich exotic nuclei. The effective single-particle energies calculated using GXPF1 also indicated a significant energy gap between the $\nu p_{1/2}$ and $\nu f_{5/2}$ orbitals, and a new magic number at $N=34$ was predicted for the Ti and Ca isotopes. The systematic variation in $E(2_1^+)$ for the even-even Ti isotopes does not bear out this possibility; in fact, the experimental $E(2_1^+)$ value in $^{56}\text{Ti}_{34}$ falls midway between the GXPF1 and KB3G predictions [9].

The β -decay properties of $^{54,55,56}\text{Sc}$ reported herein have been compared to the results of shell model calculations using the GXPF1 interaction, as was done in similar investigations of the neutron-rich V [11] and Ti [12] nuclides. The calculations were performed using the codes OXBASH [22] and CMICHSM [23]. The calculated low-energy level structures for the odd-odd parents $^{54,56}\text{Sc}$ are presented in Fig. 12. The ground-state of ^{54}Sc is predicted to have spin and parity 4^+ and is separated by only 123 keV from the first excited state, calculated to have $J^\pi=3^+$. A very different low-energy structure is expected for ^{56}Sc . The ground state of ^{56}Sc is calculated to have spin and parity 1^+ , with a doublet of states with $J^\pi=2^+, 6^+$ calculated to lie at an energy of ~ 500 keV above the ground state. The following discussion focuses on the significant changes to the low-energy structure and the β -decay properties of these nuclides resulting from the addition of two neutrons in going from ^{54}Sc to ^{56}Sc .

Since the energy separation between the two lowest states calculated in ^{54}Sc is only 123 keV, the β decay properties of ^{54}Sc were calculated assuming $J^\pi=3^+$ or 4^+ for the ground state of this nuclide. A calculated half-life of 724 ms (1.92 s) was obtained for the β -decay of the $J^\pi=3^+$ ($J^\pi=4^+$) state. These half-lives were multiplied by a factor of 2 to account for the known reduction in calculated Gamow-Teller strength in the full pf -shell model space when compared to experiment [10]. For both potential spin and parity assignments to the ground state of ^{54}Sc , the present shell model calculations predict a much longer half-life than the experimental value of 360 ± 60 ms reported here. The calculated β -branching ratios to excited states in ^{54}Ti are similar for these two pos-

sible spin assignments. Considering only direct β decays to states in ^{54}Ti below 3 MeV, the potential $3^+, 4^+$ ground states of the ^{54}Sc parent both preferentially populate the 4_1^+ state in ^{54}Ti , with calculated branches of 12% and 17%, respectively. It is, therefore, difficult to make any assumptions on the spin and parity of the ^{54}Sc ground state based on a comparison between the shell model results with the GXPF1 interaction and the experimental data.

The presence of an $E2$ isomeric transition at 110 keV in ^{54}Sc provides additional insight into the low-energy structure of the ^{54}Sc parent. The calculated position of the first 1^+ level in ^{54}Sc , which has a $(\pi f_{7/2})^1(\nu p_{3/2})^4(\nu f_{5/2})^1$ composition, compared to the ground-state doublet, which is most likely $(\pi f_{7/2})^1(\nu p_{3/2})^4(\nu p_{1/2})^1$, furthers the understanding of the relative position and energy separation of the $\nu f_{5/2}$ and $\nu p_{1/2}$ single-particle orbitals. If the monopole migration of the $\nu f_{5/2}$ is overestimated with the GXPF1 interaction, as suggested in Ref. [9], the 1^+ state may reside much closer to the ground state and could give rise to the observed $E2$ isomeric transition.

^{56}Sc differs from ^{54}Sc by two neutrons, and the unpaired neutron is expected to occupy the $\nu f_{5/2}$ orbital. A 1^+ ground state is predicted for ^{56}Sc from the shell model calculations employing the GXPF1 interaction. Similar to the situation in ^{54}Sc , the separation between the $\nu f_{5/2}$ and $\nu p_{1/2}$ single-particle states is expected to be smaller than that reflected in the GXPF1 results given in Fig. 12. A condensed low-energy spectrum for ^{56}Sc may produce several isomers; both high- and low-spin β -decaying states have been observed in ^{56}Sc . The low-spin isomer decays primarily to the ground state of ^{56}Ti , with an apparent branching ratio of $(62\pm 15)\%$. The results of shell model calculations using the GXPF1 interaction predict a 42% β branch for the ^{56}Sc 1^+ decay to the ground state of ^{56}Ti . Based on direct feeding to the first 6^+ state in the daughter ^{56}Ti , the spin and parity of the high-spin β -decaying state in ^{56}Sc have been tentatively assigned values of $(6^+, 7^+)$. The shell model calculations performed here predicted a 68% β -decay branching for the ^{56}Sc 6^+ decay to the first excited 6^+ state in ^{56}Ti , and this was the only direct feeding to excited states in ^{56}Ti below 4 MeV.

The calculated β -decay half-lives for the 1^+ and 6^+ states are 16 ms (35 ± 5 ms) and 110 ms (60 ± 7 ms), respectively, where the corresponding experimental numbers are given in parentheses. For both calculations, a Q_β value of 13.7 MeV [19] was used, as the energy separation and order of the high- and low-spin β -decaying isomers is unknown. The calculated half-lives were again corrected by a factor of 2 to account for the reduction in calculated Gamow-Teller strength for neutron-rich nuclides in this region. The experimental half-lives for the two β -decaying isomers in ^{56}Sc fall within a factor of 2 of the shell model results.

The three isomeric γ rays observed in ^{56}Sc have not been placed. The expected compression of the low-energy spectrum of ^{56}Sc shown in Fig. 12 may result in isomeric transitions populating either of the two β -decaying states. The low statistics in the current experiment did not permit the analysis of coincidence relationships between the three γ rays. Additional data on the time evolution of each of the isomeric γ rays would also help to place these transitions in the level structure of the ^{56}Sc parent.

The ^{55}Sc ground state is predicted to have $7/2^-$ quantum numbers and follows the systematic trend of other odd- A , $\pi f_{7/2}$ nuclei. The deduced half-life of 115 ± 15 ms compares well with the shell model result of 156 ms. The largest β -decay branch, calculated here to be 31%, is to the lowest $5/2^-$ level in the daughter ^{55}Ti . The ground-state spin and parity of ^{55}Ti have been proposed to be $(3/2, 5/2, 7/2)^-$ [12], based on the β -decay branchings observed experimentally in the decay of $^{55}\text{Ti} \rightarrow ^{55}\text{V}$. The suggestion of direct β feeding to the ^{55}Ti ground state, even if it is only based on the limited delayed γ -ray data presented here for the decay of ^{55}Sc , would tend to support a $5/2^-$ or $7/2^-$ ground state for ^{55}Ti .

B. Monopole migration of $\nu f_{5/2}$ based on ground-state spin and parity assignments

Using the tentative spin and parity assignments for the $^{54,56}\text{Si}$, ^{55}Ti , and $^{56,58}\text{V}$ isotopes, the monopole migration of the $\nu f_{5/2}$ state with removal of protons from the $\pi f_{7/2}$ level can be described. The spins and parities for the ground states of Sc, Ti, and V nuclei around the $N=32$ subshell closure, together with schematic neutron single-particle levels, are shown in Fig. 13. There is substantial evidence for the existence of a subshell closure located at $N=32$ as discussed above. Working from this subshell closure, the extreme single-particle model can be used to infer the proton and neutron orbitals that couple to produce the observed ground state spins and parities.

Starting in the ^{21}Sc isotopes, the odd proton is located in the $\pi f_{7/2}$ state, as evidenced by the ground-state spins and parities of odd- A Sc isotopes. Coupling this proton to an odd neutron in the $\nu f_{5/2}$ orbital results in a range of spin and parity of $(1-6)^+$, while coupling an $f_{7/2}$ proton to an odd neutron in the $\nu p_{1/2}$ state would lead to spin and parity of 3^+ or 4^+ . The ground-state spin and parity of ^{54}Sc have been tentatively identified as $(3,4)^+$. Nordheim rules [24,25] argue against the coupling of a proton in the $\pi f_{7/2}$ to a neutron in the $\nu f_{5/2}$ level resulting in a $(3,4)^+$ ground state. This suggests that the 33rd neutron occupies the $\nu p_{1/2}$ orbital. The tentative spin and parity of 1^+ in ^{56}Sc in a single-particle picture is only possible with the placement of the 35th neutron in the $\nu f_{5/2}$ level. From the schematic neutron levels, it is seen that the $\nu f_{5/2}$ level is located above the $\nu p_{1/2}$ state in the ^{21}Sc isotopes.

In the ^{23}V isotopes, the odd proton is still located in the $\pi f_{7/2}$ orbit. Both $^{56,58}\text{V}$ have been assigned 1^+ ground states, placing the 33rd and 35th neutrons in the $\nu f_{5/2}$ state and suggesting that the $\nu f_{5/2}$ orbital is lower than the $\nu p_{1/2}$ level in ^{23}V nuclei.

The β decay of the odd-even nucleus ^{55}Ti has also been studied [12] and, while the spin and parity have not been firmly established, the complex feeding observed in the β decay of ^{55}Ti is not indicative of a dominant $\nu p_{1/2}$ single-particle configuration for the ^{55}Ti ground state. The new results reported here on the β decay of ^{55}Sc into the low-energy levels of ^{55}Ti suggest a significant β -decay feeding the ground state of ^{55}Ti . Assuming $J=7/2$ for the ^{55}Sc parent state, a β -decay branch directly to the daughter ground state

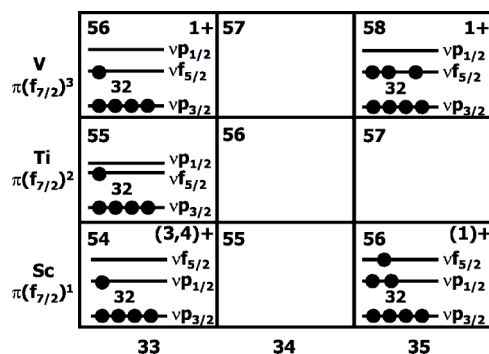


FIG. 13. Spin and parities for selected ^{23}V and ^{21}Sc isotopes with schematic neutron single-particle levels. Energy spacings are not to scale.

also suggests that the ground-state spin of ^{55}Ti is greater than $1/2$.

While the $\nu f_{5/2}$ and $\nu p_{1/2}$ single-particle level orderings, inferred from the spin and parity assignments to the ground states of odd-odd $^{54,56}\text{Sc}$ and $^{56,58}\text{V}$ isotopes, agree with shell model calculations, the present data on the low-energy levels of the neutron-rich Sc and Ti isotopes do not support a large energy separation between the $\nu f_{5/2}$ and $\nu p_{1/2}$ orbitals predicted using the GXPF1 interaction. As noted in Ref. [9], a reduction of ≈ 0.8 MeV in the single-particle energy of the $\nu f_{5/2}$ state would account for the absence of an $N=34$ shell closure. To preserve calculated levels in other nuclei, a weaker monopole interaction should be considered to account for the slower rise in energy of the $\nu f_{5/2}$ state with the removal of protons from the $\pi f_{7/2}$ orbit [8] and a location of the first 2^+ state in ^{54}Ca around 4 MeV. However, the monopole migration of the $\nu f_{5/2}$ state is expected to continue with the removal of the last two protons from the $\pi f_{7/2}$ orbital in the ^{20}Ca isotopes. Further investigation of the low-energy level structure of neutron-rich Ca nuclei is warranted to determine if a $\nu f_{5/2}$ - $\nu p_{1/2}$ energy gap dominates at $N=34$, resulting in a shell closure.

V. SUMMARY

The low-energy levels of neutron-rich $^{54,55,56}\text{Ti}$ have been studied through the β decay of the parent nuclides $^{54,55,56}\text{Sc}$, respectively. The systematic variation in the $E(2^+)$ values for the even-even ^{22}Ti isotopes reveal a peak at $N=32$ indicative of a subshell closure. This increase is similar to the increase in $E(2^+)$ at $N=32$ observed for the ^{20}Ca and ^{24}Cr isotopes. Evidence for a shell closure at $N=34$, predicted for the Ti isotopes by shell model calculations carried out using the new pf -shell interaction GXPF1, was not observed. Based on β -decay branching ratios for the $^{54,56}\text{Sc}$ decays, tentative spin and parity assignments were proposed for the odd-odd parent nuclei. A survey of the spin-parity assignments of the ground states of the odd- A and odd-odd nuclides in this region was used to analyze, in a schematic way, the monopole migration of the $\nu f_{5/2}$ orbital. While there is evidence that the $\nu f_{5/2}$ - $\nu p_{1/2}$ level ordering changes between ^{23}V and ^{21}Sc ,

there is no substantial proof that a large energy gap between the $\nu f_{5/2}$ and $\nu p_{1/2}$ develops for the ${}_{22}\text{Ti}$ isotopes. Support for this conclusion is found in the systematic variation of $E(2_1^+)$ for the even-even Ti isotopes and the presence of isomeric transitions in ${}^{54,56}\text{Sc}$, which suggests a more compressed low-energy spectrum than predicted by the shell model results reported here using the GXPF1 interaction. It is important to continue to track the progression of the monopole migration to the ${}_{20}\text{Ca}$ isotopes, which have no $f_{7/2}$ protons. The “full” monopole shift of the $\nu f_{5/2}$ orbital may lead to a large gap in the $\nu f_{5/2} - \nu p_{1/2}$ effective single particle energies, still producing a shell closure at $N=34$ for the Ca isotopes.

ACKNOWLEDGMENTS

This work was supported in part by the National Science Foundation Grants Nos. PHY-01-10253, PHY-97-24299, PHY-01-39950, and PHY-02-44453, and by the U.S. Department of Energy, Office of Nuclear Physics, under Contract No. W-31-109-ENG-38. The authors would like to thank the NSCL operations staff for providing the primary and secondary beams for this experiment. The authors also thank the members of the NSCL γ group who helped with the set up of the SeGA detector array. The thick DSSD used for the ${}^{56}\text{Sc}$ β -decay measurements was provided by K. Rykaczewski (ORNL).

-
- [1] X. L. Tu, X. G. Zhou, D. J. Vieira, J. M. Wouters, Z. Y. Zhou, H. L. Seifert, and V. G. Lind, *Z. Phys. A* **337**, 361 (1990).
- [2] A. Huck, G. Klotz, A. Knipper, C. Mieke, C. Richard-Serre, G. Walter, A. Poves, H. L. Ravn, and G. Marguier, *Phys. Rev. C* **31**, 2226 (1985).
- [3] F. Tondeur, CERN Report No. 81-09, 1981, p. 81.
- [4] J. I. Prisciandaro, P. F. Mantica, B. A. Brown, D. W. Anthony, M. W. Cooper, A. Garcia, D. E. Groh, A. Komives, W. Kumarasiri, P. A. Lofy, A. M. Oros-Peusquens, S. L. Tabor, and W. Wiedeking, *Phys. Lett. B* **510**, 17 (2001).
- [5] D. E. Appelbe *et al.*, *Phys. Rev. C* **67**, 034309 (2003).
- [6] R. V. F. Janssens *et al.*, *Phys. Lett. B* **546**, 55 (2002).
- [7] M. Honma, T. Otsuka, B. A. Brown, and T. Mizusaki, *Phys. Rev. C* **65**, 061301(R) (2002).
- [8] M. Honma, T. Otsuka, B. A. Brown, and T. Mizusaki, *Phys. Rev. C* **69**, 034335 (2004).
- [9] S. N. Liddick *et al.*, *Phys. Rev. Lett.* **92**, 072502 (2004).
- [10] A. Poves, J. Sanchez-Solano, E. Caurier, and F. Nowacki, *Nucl. Phys.* **A694**, 157 (2001).
- [11] P. F. Mantica *et al.*, *Phys. Rev. C* **67**, 014311 (2003).
- [12] P. F. Mantica, B. A. Brown, A. D. Davies, T. Glasmacher, D. E. Groh, M. Horoi, S. N. Liddick, D. J. Morrissey, A. C. Morton, W. F. Mueller, H. Schatz, A. Stolz, and S. L. Tabor, *Phys. Rev. C* **68**, 044311 (2003).
- [13] D. J. Morrissey, B. M. Sherrill, M. Steiner, A. Stolz, and I. Wiedenhöver, *Nucl. Instrum. Methods Phys. Res. B* **204**, 90 (2003).
- [14] J. I. Prisciandaro, A. C. Morton, and P. F. Mantica, *Nucl. Instrum. Methods Phys. Res. A* **505**, 140 (2003).
- [15] W. F. Mueller, J. A. Church, T. Glasmacher, D. Gutknecht, G. Hackman, P. G. Hansen, Z. Hu, K. L. Miller, and P. Quirin, *Nucl. Instrum. Methods Phys. Res. A* **466**, 492 (2001).
- [16] O. Sorlin *et al.*, *Nucl. Phys.* **A632**, 205 (1998).
- [17] T. Dörfler *et al.*, *Phys. Rev. C* **54**, 2894 (1996).
- [18] R. Grzywacz *et al.*, *Phys. Rev. Lett.* **81**, 766 (1998).
- [19] G. Audi, A. H. Wapstra, and C. Thibault, *Nucl. Phys.* **A729**, 337 (2003).
- [20] B. Fornal *et al.*, *Phys. Rev. C* **70**, 064304 (2000), the following paper.
- [21] T. Otsuka, R. Fujimoto, Y. Utsuno, B. A. Brown, M. Honma, and T. Mizusaki, *Phys. Rev. Lett.* **87**, 082502 (2001).
- [22] B. A. Brown, A. Etchegoyen, and W. D. M. Rae, computer code OXBASH, MSU-NSCL Report No. 524, 1998.
- [23] M. Horoi, B. A. Brown, and V. Zelevinsky, *Phys. Rev. C* **67**, 034303 (2003).
- [24] L. Nordheim, *Rev. Mod. Phys.* **23**, 322 (1951).
- [25] M. H. Brennan and A. M. Bernstein, *Phys. Rev.* **120**, 927 (1960).